ADVANCED MATERIALS TECHNOLOGIES
www.advmattechnol.de

Anisotropic Temperature Dependent Band Shift in Layered Black Phosphorus

*Jingwei Dong, Runze Liu, Yi Lian, Shengtao Cui, Zhe Sun, and Zhongwei Chen**

Temperature acts as a control lever for the electronic band structure in black phosphorus (BP), significantly influencing its device performance. While the effects of electron-phonon coupling and lattice thermal expansion on the temperature-dependent band gap are well understood, there have been no reports on the electronic band as a function of temperature. Additionally, although black phosphorus is well-known for its significant anisotropic optoelectronic properties, there is comparatively less understanding regarding how various lattice constants affect the electronic band in response to temperature changes. Herein, temperature dependence of the valence band of BP has been measured by angle-resolved photoelectron spectroscopy (ARPES) and the band shifts are quantitatively characterized. The band shift along the k_x direction is larger than that along the k_y direction upon heating from 10 to 200 K even if changing the photon energy. It is certified that the band shifts are primarily attributed to the lattice expansion across different crystal orientations, as determined by density functional theory (DFT) calculations. This study investigates the anisotropic temperature dependence of the electronic band shift in black phosphorus, revealing the underlying mechanisms. These findings will be instrumental in guiding the rational design of BP-based devices tailored for operation across a range of temperatures.

1. Introduction

Black phosphorus, a rising star among layered semiconductors, has garnered significant attention due to its distinctive optical and electronic properties.[1–7] BP shows anisotropic in plane band structure because of the puckering atomic structure along the *x* axis.[1] It retains the direct band gap, which is tunable from 0.3 eV in the bulk to 1.5 eV in the monolayer.[2,3] Furthermore, BP-based field-effect transistors exhibit an on/off ratio of 10^5 and a hole-dominated carrier mobility of 10^3 cm^2 Vs, respectively.[4–7] Most interestingly, the electronic properties of black phosphorus can be modulated not only by electric fields and surface dipoles but also by temperature.[4,8–13] The bandgap of BP is sensitive to temperature.[13–15] Villegas et al ascribed the abnormal increase of thick BP band gap with temperature to the electron-phonon scattering and thermal expansion.[15] Temperature dependent carrier mobility of BP has also been reported: below 100 K, the carrier mobility remains unaffected and the electron-ionized impurity scattering is proposed to dominate; between 100 and 300 K, the carrier mobility decrease with temperature, which is attributed to electron-phonon scattering.[4]

The electronic band structure of black phosphorus is indeed a fundamental aspect for understanding its electronic and optoelectronic properties, and it has been extensively studied through theoretical calculations[6,16–18] and angle-resolved photoelectron spectroscopy.[19–23] For example, the thickness dependent electronic band dispersion has also been studied as a function of layers.[6,16,22] Most recently, Margot and coworkers measured the electronic band structure of 2–9 layer BP with micro-focused ARPES, confirming the decrease of hole effective mass with layers along *y* and the almost independence in *x* direction.[22] In analogy to the temperature-dependent band gap and thickness-dependent hole effective mass in BP, a sizable valence band evolution may be expected upon heating/cooling. In addition, the in-plane band dispersion of black phosphorus exhibits anisotropy. It is intriguing to reveal whether the temperature dependence of the valence band mirrors this anisotropy. Most importantly, it is essential to clarify the decisive factors that govern the evolution of the valence band with temperature.

J. Dong, Z. Chen
Power Battery & Systems Research Center, Dalian Institute of Chemical Physics
Chinese Academy of Sciences
Dalian 116023, P. R. China
E-mail: zwchen@dicp.ac.cn

J. Dong, Z. Chen
State Key Laboratory of Catalysis
Dalian Institute of Chemical Physics
Chinese Academy of Sciences
Dalian 116023, P. R. China

R. Liu
School of Science
Dalian Jiaotong University
Dalian 116028, P. R. China

Y. Lian
Institute of Atomic and Molecular Physics
Jilin University
Changchun 130012, P. R. China

S. Cui, Z. Sun
National Synchrotron Radiation Laboratory
University of Science and Technology of China
Hefei 230029, P. R. China

The ORCID identification number(s) for the author(s) of this article can be found under https://doi.org/10.1002/admt.202402146

DOI: 10.1002/admt.202402146

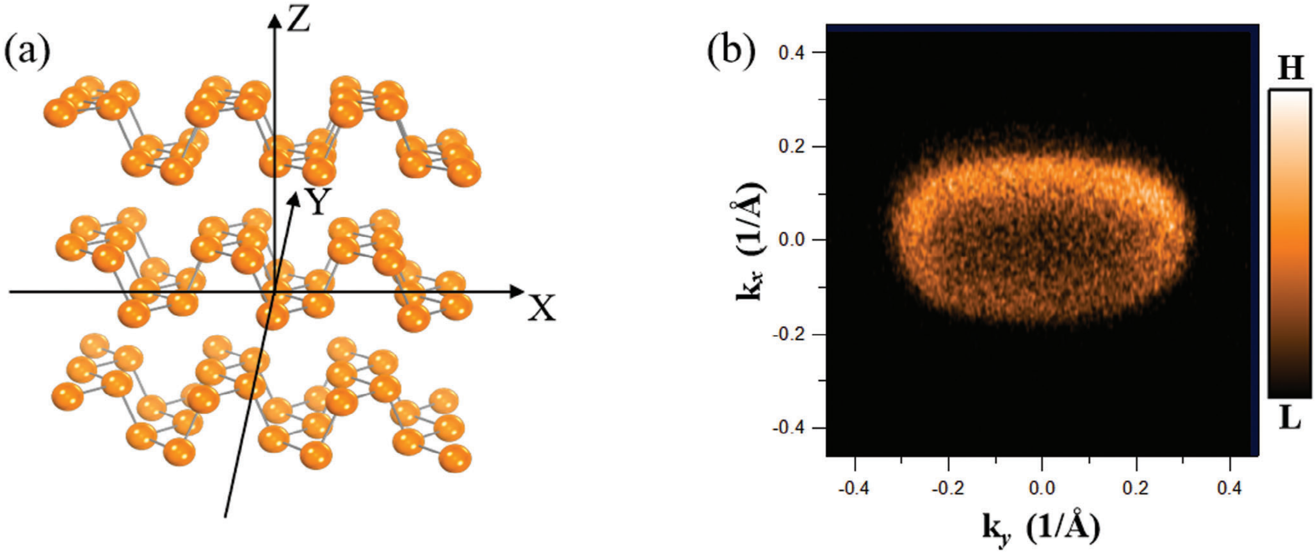

Figure 1. a) Layered crystal structure of black phosphorus. b) Constant-energy contour acquired by p-polarized light ($h\nu = 21$ eV) at the binding energy of 0.8 eV.

To address the above significant issues in BP, we have decoupled the effects of lattice expansion from three distinct crystal orientations on the valence band evolution within the k_x and k_y momentum space. We observed that the band shift along the k_x direction is roughly 0.06 eV when heated from 10 to 200 K, while the band shift along the k_y direction is only 0.03 eV, regardless of changes in photon energy. Together with DFT calculations, the anisotropic lattice expansions from three crystal orientations were revealed. This systematic investigation of temperature effect on the valence band shift in BP not only identifies the anisotropic temperature dependence but also uncovers the underlying mechanisms. These insights will aid in understanding temperature-dependent phenomena in BP and serve as a model for studying the temperature effects in other anisotropic 2D materials.

2. Results and Discussion

Layered BP exhibits a distinctive crystal structure characterized by a puckered configuration along the x-axis, a result of the sp^3 hybridization of phosphorus atoms as shown in **Figure 1**a. This structural feature gives rise to pronounced anisotropy in its in-plane optoelectronic and electronic properties.[1,17,21] The elliptical pockets in the constant energy contour at a binding energy of 0.8 eV, as shown in Figure 1b, allow us to identify the two high-symmetry directions, k_x and k_y, and also reveal the anisotropic electronic band dispersion along the two perpendicular in-plane directions.

In order to reveal the electronic band structure evolution at the BP crystal surface with temperature, the valence bands of BP along k_x and k_y directions at 10 and 200 K have been measured using 21 eV photons first (**Figure 2**). The inelastic mean free path of emitted photoelectrons varies with their kinetic energy.[10,24] Using excitation light with photon energy of 21 eV, the corresponding probing depth is close to the topmost layers. Compared to the valence band maximum (VBM) in Figure 2a, the top appears to descend in energy space in Figure 2b. In order to quantitatively analyze the evolution of valence band with temperature, energy distribution curves (EDCs) at 0 Å^{-1} (momentum range; −0.01–0.01 1/Å) at 10 and 200 K have been extracted, respectively. As shown in Figure 2c, the VBM is ≈ −0.025 eV at 10 K and −0.085 eV at 200 K. This indicates a band shift of 0.06 eV upon heating from 10 K to 200 K. Similarly, the valence band along the k_y direction also occurs a band shift of 0.03 eV with an ≈200 K increase in temperature (Figure 2d–f). The observed band downshift is both evident and reliable, given the total convolved energy resolution of 15 meV. The shift value along the k_x direction is nearly twice that of the value along the k_y direction. More detailed band shifts along the k_y direction with temperature are shown in Figure S1 (Supporting Information).

To determine whether the observed band shift phenomenon is exclusive to the surface of the BP crystal, further investigation is required. Tuning the photon energy from 21 to 7.2 eV, the corresponding probing depth changes from the near topmost layers to the bulk of the crystal. Identical measurements on the temperature dependence of the valence band along the k_x and k_y directions are also performed by 7.2 eV photon energy (**Figure 3**). The VBM is ≈ −0.090 eV at 10 K and −0.140 eV at 200 K, which represents a band downshift of 0.05 eV from 10 to 200 K (Figure 3c). In terms of the valence band along the k_y direction, it has a band downshift of 0.035 eV upon heating (Figure 3f). The shift value along the k_x direction is larger than that along the k_y direction as well. These findings suggest that the band downshift occurs not only at the surface but also throughout the bulk of the BP crystal. According to the previous studies on the anomalous temperature dependence of the band gap in bulk black phosphorus,[13,15] the lattice expansion and adiabatic electron−phonon coupling may lead to a gap opening of a few meV. Following the analysis of the temperature-dependent band gap, we will next systematically analyze each influencing factor on the band downshift individually.

Typically, heating results in an increase in lattice constants. Figure S2 (Supporting Information) shows the single-crystal X-ray diffraction (XRD) patterns of BP with temperature (100,

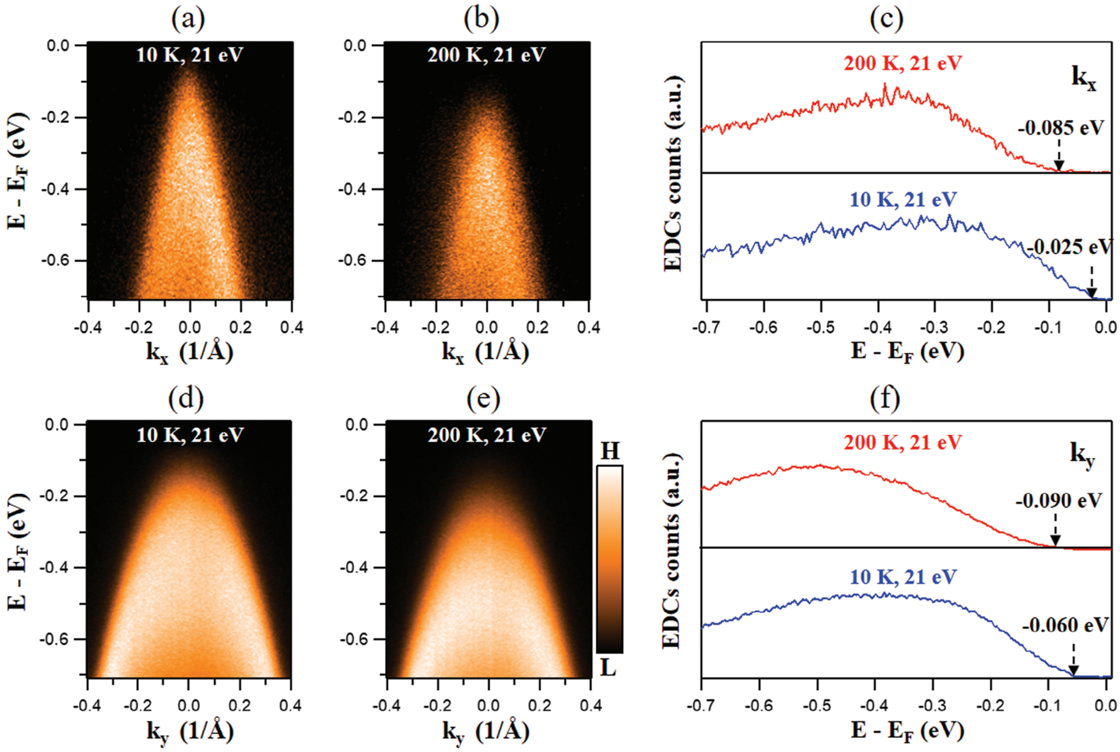

Figure 2. a,b) Photoelectron intensity maps recorded along the k_x direction with s-polarized light at 10 and 200 K using 21 eV photon energy, respectively. c) Energy distribution curves at 0 Å^{-1} (momentum range; −0.01–0.01 1/Å) at 10 K (blue curve) and 200 K (red curve), respectively. The black arrows indicate the valence band maximum. d–f) The corresponding scenarios along the k_y direction with p-polarized light.

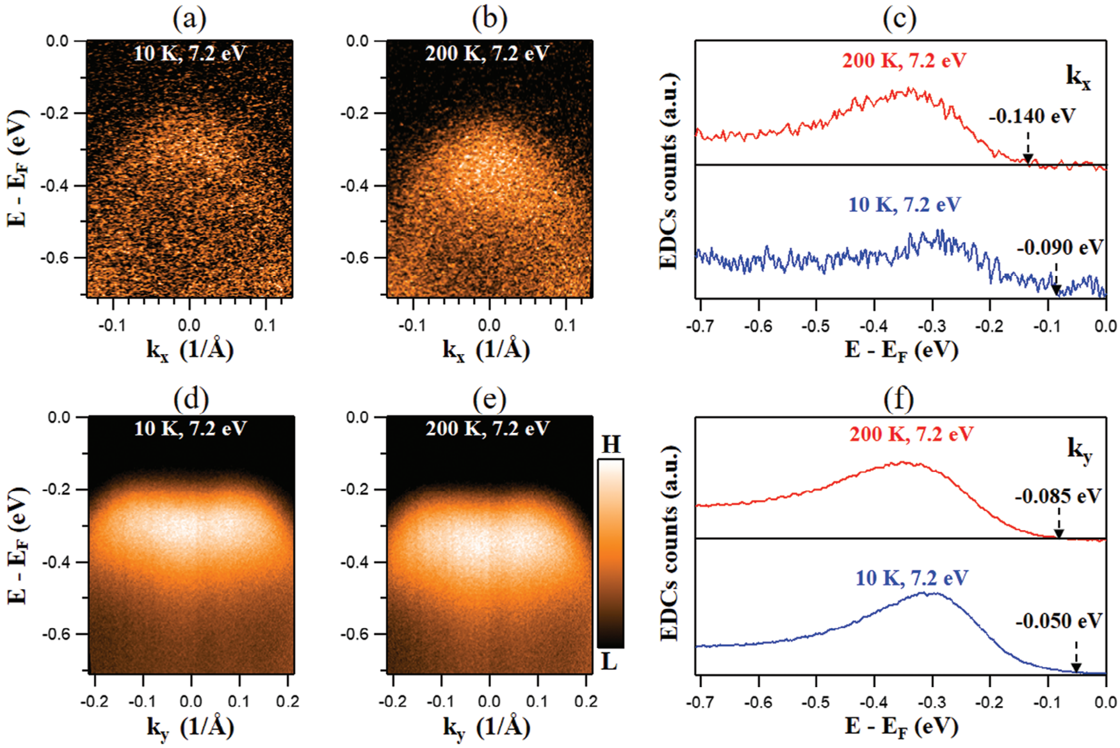

Figure 3. a–c) Photoelectron intensity maps and EDCs recorded along the k_x direction with s-polarized light at 10 and 200 K using 7.2 eV photon energy, respectively. d–f) the corresponding scenarios along the k_y direction with p-polarized light.

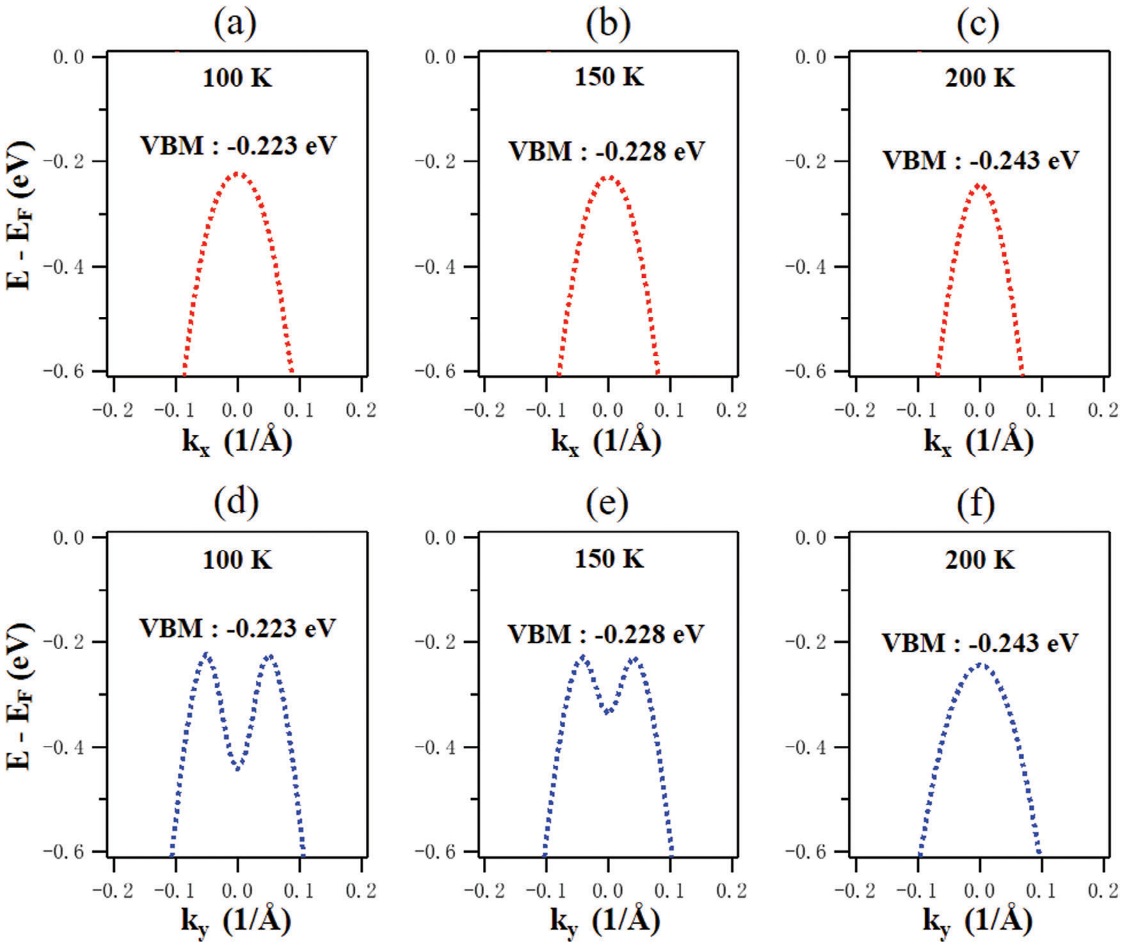

Figure 4. Calculated valence bands of BP along the k_x and k_y directions as a function of temperature. VBMs are shown in the Figure. Different temperatures correspond to the different lattice constants.

150 and 200 K). The extracted lattice constants (100 K: a = 3.295(0.033), b = 10.386(0.103), c = 4.302(0.043); 150 K: a = 3.333(0.048), b = 10.501(0.147), c = 4.356(0.061); 200 K: a = 3.335(0.052), b = 10.565(0.158), c = 4.403(0.069)) are shown in Figure S2a (Supporting Information). By these parameters, first-principles calculations were performed to reveal the temperature-dependent band shift in BP. **Figure 4** shows the valence bands of BP in three expanding directions using DFT calculations. The VBMs along the k_x and k_y directions downshift by 0.020 eV from 100 to 200 K, aligning well with the experimental band shift along the k_y direction shown in Figure S1 (Supporting Information). This indicates that the band downshift along the k_y direction mainly due to the lattice expansion. The factors contributing to the band downshift along the k_x direction likely include elements beyond lattice expansion. It's important to note that the electronic band dispersion in BP is k_z-dependent.[22] Consequently, the calculated band dispersion along the k_y direction, shown in Figure 4d–f, closely matches the experimental maps obtained with 7.2 eV photons, as seen in Figure 3d,e, rather than those obtained with 21 eV photons, as depicted in Figure 2d,e.

Although the role of lattice expansion in causing the band downshift in BP is well established, the precise lattice factors that significantly influence the band shift during heating are still not fully understood. To clarify the contributions of lattices a, b and c upon heating, first-principles calculations with various lattice constants were employed. As shown in **Figure** 5a,b, we increased the value of lattice parameter a to 3.333 and 3.335 Å from its original value of 3.295 Å (Figure S2, Supporting Information), while keeping the lattice parameters b and c invariant. Compared to the original VBM (−0.223 eV; Figure 4a), the band occurs a downshift of roughly 0.030 eV (−0.252 eV; Figure 5b). On the contrary, the band occurs an upshift of roughly 0.040 eV (−0.182 eV; Figure 5d) when we increased the value of lattice parameter b to 10.501 and 10.565 Å from its original value of 10.386 Å (Figure S2, Supporting Information) while keeping the lattice parameters a and c invariant. Similarly, as shown in Figure 5e,f, keeping the lattice parameters a and b invariant but increasing the value of lattice parameter c to 4.356 and 4.403 Å from its original value of 4.302 Å (Figure S2, Supporting Information), the band experienced an upshift of 0.047 eV. Changing the k_x to the k_y direction, the same band shift is observed, as shown in Figure 5g–l. Based on the above results, we can conclude that lattice expansion in the a direction positively contributes to the band downshift upon heating, while expansions in the b and c directions have a negative impact. Returning to the discussion of the shift differences

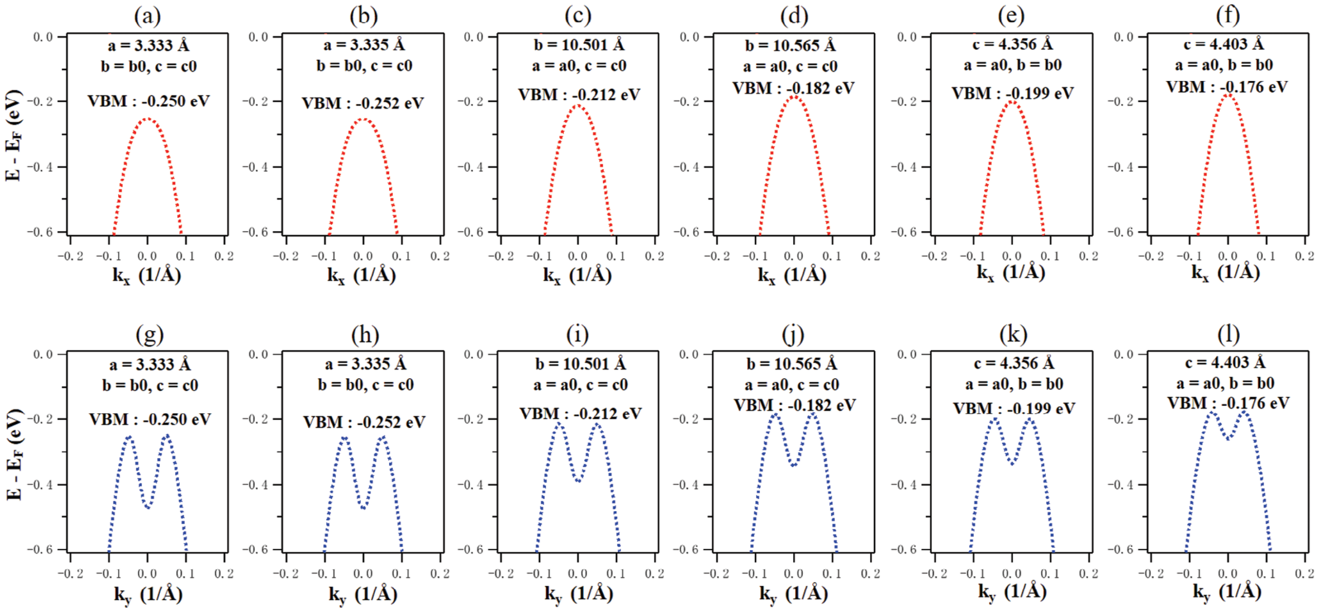

Figure 5. Calculated valence bands of BP along the k_x and k_y directions as a function of lattice constants. VBMs and lattice constants we used are illustrated in the Figure.

between the k_x and k_y directions, we revealed that the experimental and theoretical results along the k_y direction are consistent. However, the theoretical values are smaller than those obtained from experimental measurements.

Temperature variation may lead to the change of defect density and electron-phonon scattering.[4,13,25] The most likely defect in black phosphorus crystals is the substitution of phosphorus atoms with tin (Sn) atoms. X-ray Photoelectron Spectroscopy (XPS; Figure S3, Supporting Information) provides the P2*p* orbital and Sn3*d* orbital at 100 and 300 K, respectively. The concentration of Sn3d remains virtually invariant. BP samples were fabricated at a temperature as high as 860 K. We believe that the concentration of defects does not change in the 10–200 K range in the UHV condition. Therefore, electron-defect scattering will remain the same in this whole temperature range in the current work. On the other hand, anisotropic electron-phonon scattering in different high symmetric directions in BP has been reported.[26] In anisotropic BP, the dielectric constant along the armchair direction is higher than that along the zigzag one,[27] suggesting the polarization, in other words, the electron-phonon scattering, is different. The phonon density of states along the zigzag direction is different from that along the armchair direction.[28] Phonon-dressed electronic band structure has frequently been reported in both 2D and 3D materials.[29,30] These are consistent with the anisotropic effect of electron-phonon scattering on the band downshift in our temperature dependent ARPES measurements, but future work is needed to quantitatively assess the relative contribution.

3. Conclusion

In conclusion, valence bands along k_x and k_y directions in BP have been investigated by means of photon energy dependent ARPES as a function of temperature. The band shift was observed upon heating, and the value along the k_x direction is larger than that along the k_y direction. Combining DFT calculations, we revealed that the band downshift along the k_y direction is primarily attributed to the expansion of lattice parameter a upon heating. In contrast, the shift along the k_x direction is likely due to electron-phonon interactions in addition to lattice expansion. Gaining an understanding of the anisotropic temperature dependence of electronic band shifts in black phosphorus is crucial for the precise manipulation of its optical and electronic properties through temperature control. Moreover, this understanding could be instrumental in optimizing the performance of other anisotropic 2D materials.

4. Experimental Section

All ARPES experiments were carried out at beamline BL13U of National Synchrotron Radiation Laboratory (NSRL) in Hefei, China. The photon energy can be tuned from 7 to 35 eV. The extreme ultraviolet light shined onto the BP surface with an angle of 50 degrees and the beam spot size (H × V) at the sample position was ≈0.3 × 0.3 mm^2. The light polarization was tuned by the horizontal movement of the elliptical polarization undulator (EPU), producing p/s-polarized (the electric field is parallel/vertical to the incident plane) beam. The photoelectrons were collected with a Scienta DA30 analyzer equipped with electrostatic lens allowing Fermi surface mapping without sample rotation. The total convolved energy and angle resolutions were 15 meV and 0.2° respectively. P-type single crystalline BP (thickness: 0.2 mm, lateral dimensions: 1 × 1 mm^2; Nanjing MKNANO Tech. Co.,Ltd. (www.mukenano.com)) were cleaved at 10 K and measured at a base pressure of 8×10^{-11} Torr. The energy zero in all photoelectron spectra was set at the Fermi level that was referenced to a copper plate in electrical contact with the samples. No charging effect is observed during the measurements.

All DFT calculations were performed using Materials Studio 2017 with the Doml3 software.[31,32] A generalized gradient approximation was used with the Perdew-Burke-Ernzerhof exchange correlation function.[33] The following configurations were chosen for the geometry optimizations:

convergence standards of 10^{-5} Ha on energy, 2×10^{-3} Ha/Å on the force, and 5×10^{-3} Å on displacement. The Brillouin zone was sampled using a $4 \times 1 \times 3$ gamma-centered Monkhorst-Pack grid.[34–36]

Supporting Information

Supporting Information is available from the Wiley Online Library or from the author.

Acknowledgements

This work was supported by the Natural Science Foundation of China (Grant No. 22409194), the Energy Revolution S&T Program of Yulin Innovation Institute of Clean Energy, (Grant No. YICE E411060316), and the Strategic Priority Research Program of the Chinese Academy of Sciences (Grant No. XDB0600000, XDB0600200).

Conflict of Interest

The authors declare no conflict of interest.

Data Availability Statement

The data that support the findings of this study are available from the corresponding author upon reasonable request.

Keywords

anisotropic temperature dependence, ARPES, black phosphorus, electronic band shift, lattice thermal expansion

Received: December 20, 2024
Revised: January 26, 2025
Published online:

---

[1] M. Buscema, D. J. Groenendijk, S. I. Blanter, G. A. Steele, H. S. J. van der Zant, A. Castellanos-Gomez, *Nano Lett.* **2014**, *14*, 3347.
[2] H. Liu, A. T. Neal, Z. Zhu, Z. Luo, X. Xu, D. Tomanek, P. D. Ye, *ACS Nano* **2014**, *8*, 4033.
[3] F. Xia, H. Wang, Y. Jia, *Nat. Commun.* **2014**, *5*, 4458.
[4] L. Li, Y. Yu, G. J. Ye, Q. Ge, X. Ou, H. Wu, D. Feng, X. H. Chen, Y. Zhang, *Nat. Nanotechnol.* **2014**, *9*, 372.
[5] R. A. Doganov, E. C. T. O'Farrell, S. P. Koenig, Y. Yeo, A. Ziletti, A. Carvalho, D. K. Campbell, D. F. Coker, K. Watanabe, T. Taniguchi, A. H. Castro Neto, B. Ozyilmaz, *Nat. Commun.* **2015**, *6*, 6647.
[6] J. Qiao, X. Kong, Z.-X. Hu, F. Yang, W. Ji, *Nat. Commun.* **2014**, *5*, 4475.
[7] F. Ahmed, Y. D. Kim, Z. Yang, P. He, E. Hwang, H. Yang, J. Hone, W. J. Yoo, *Nat. Commun.* **2018**, *9*, 3414.
[8] J. Kim, S. S. Baik, S. H. Ryu, Y. Sohn, S. Park, B.-G. Park, J. Denlinger, Y. Yi, H. J. Choi, K. S. Kim, *Science* **2015**, *349*, 723.
[9] Y. Liu, Z. Qiu, A. Carvalho, Y. Bao, H. Xu, S. J. R. Tan, W. Liu, A. H. C. Neto, K. P. Loh, J. Lu, *Nano Lett.* **2017**, *17*, 1970.
[10] Z. Chen, J. Dong, C. Giorgetti, E. Papalazarou, M. Marsi, Z. Zhang, B. Tian, Q. Ma, Y. Cheng, J.-P. Rueff, A. Taleb-Ibrahimi, L. Perfetti, *2D Mater.* **2020**, *7*, 035027.
[11] S.-W. Kim, H. Jung, H.-J. Kim, J.-H. Choi, S.-H. Wei, J.-H. Cho, *Phys. Rev. B* **2017**, *96*, 075416.
[12] B. Deng, V. Tran, Y. Xie, H. Jiang, C. Li, Q. Guo, X. Wang, H. Tian, S. J. Koester, H. Wang, J. J. Cha, Q. Xia, L. Yang, F. Xia, *Nat. Commun.* **2017**, *8*, 14474.
[13] S. Huang, F. Wang, G. Zhang, C. Song, Y. Lei, Q. Xing, C. Wang, Y. Zhang, J. Zhang, Y. Xie, L. Mu, C. Cong, M. Huang, H. Yan, *Phys. Rev. Lett.* **2020**, *125*, 156802.
[14] C. Chen, F. Chen, X. Chen, B. Deng, B. Eng, D. Jung, Q. Guo, S. Yuan, K. Watanabe, T. Taniguchi, M. L. Lee, F. Xia, *Nano Lett.* **2019**, *19*, 1488.
[15] C. E. P. Villegas, A. R. Rocha, A. Marini, *Nano Lett.* **2016**, *16*, 5095.
[16] T. Vy, R. Soklaski, Y. Liang, L. Yang, *Phys. Rev. B* **2014**, *89*, 235319.
[17] X. Ling, S. Huang, E. H. Hasdeo, L. Liang, W. M. Parkin, Y. Tatsumi, A. R. T. Nugraha, A. A. Puretzky, P. M. Das, B. G. Sumpter, D. B. Geohegan, J. Kong, R. Saito, M. Drndic, V. Meunier, M. S. Dresselhaus, *Nano Lett.* **2016**, *16*, 2260.
[18] Y. Takao, A. Morita, *Physica B & C* **1981**, *105*, 93.
[19] T. Takahashi, H. Tokailin, S. Suzuki, T. Sagawa, I. Shirotani, *Phys. Rev. B* **1984**, *29*, 1105.
[20] C. Q. Han, M. Y. Yao, X. X. Bai, L. Miao, F. Zhu, D. D. Guan, S. Wang, C. L. Gao, C. Liu, D. Qian, Y. Liu, J.-f. Jia, *Phys. Rev. B* **2014**, *90*, 085101.
[21] Z. Chen, J. Dong, E. Papalazarou, M. Marsi, C. Giorgetti, Z. Zhang, B. Tian, J.-P. Rueff, A. Taleb-Ibrahimi, L. Perfetti, *Nano Lett.* **2019**, *19*, 488.
[22] F. Margot, S. Lisi, I. Cucchi, E. Cappelli, A. Hunter, I. Gutierrez-Lezama, K. Ma, F. von Rohr, C. Berthod, F. Petocchi, S. Ponce, N. Marzari, M. Gibertini, A. Tamai, A. F. Morpurgo, F. Baumberger, *Nano Lett.* **2023**, *23*, 6433.
[23] S. Zhou, C. Bao, B. Fan, H. Zhou, Q. Gao, H. Zhong, T. Lin, H. Liu, P. Yu, P. Tang, S. Meng, W. Duan, S. Zhou, *Nature* **2023**, *614*, 75.
[24] M. P. Seah, W. A. Dench, *Surf. Interface Anal.* **2004**, *1*, 2.
[25] J. V. Li, D. H. Levi, *J. Appl. Phys.* **2011**, *109*, 083701.
[26] H. Seiler, D. Zahn, M. Zacharias, P.-N. Hildebrandt, T. Vasileiadis, Y. W. Windsor, Y. Qi, C. Carbogno, C. Draxl, R. Ernstorfer, F. Caruso, *Nano Lett.* **2021**, *21*, 6171.
[27] T. Nagahama, M. Kobayashi, Y. Akahama, S. Endo, S. Narita, *J. Phys. Soc. Japan* **1985**, *54*, 2096.
[28] W. J. Andrey Chaves, J. Maassen, T. Dumitrica, T. Low, Cambridge University Press **2017**, 381.
[29] M. Puppin, S. Polishchuk, N. Colonna, A. Crepaldi, D. N. Dirin, O. Nazarenko, R. De Gennaro, G. Gatti, S. Roth, T. Barillot, L. Poletto, R. P. Xian, L. Rettig, M. Wolf, R. Ernstorfer, M. V. Kovalenko, N. Marzari, M. Grioni, M. Chergui, *Phys. Rev. Lett.* **2020**, *124*, 206402.
[30] F. Mazzola, J. W. Wells, R. Yakimova, S. Ulstrup, J. A. Miwa, R. Balog, M. Bianchi, M. Leandersson, J. Adell, P. Hofmann, T. Balasubramanian, *Phys. Rev. Lett.* **2013**, *111*, 216806.
[31] K. Zhang, Q. Wang, B. Wang, Y. Xu, X. Ma, Z. Li, *Appl. Surf. Sci.* **2019**, *479*, 360.
[32] X. Gui, Q. Zhou, S. Peng, L. Xu, W. Zeng, *Physica E Low Dimens. Syst. Nanostruct.* **2020**, *122*, 114224.
[33] J. P. Perdew, K. Burke, M. Ernzerhof, *Phys. Rev. Lett.* **1997**, *78*, 1396.
[34] H. J. Monkhorst, J. D. Pack, *Phys. Rev. B* **1976**, *13*, 5188.
[35] K. V. K. Rao, S. V. N. Naidu, L. Iyengar, *J. Am. Ceram. Soc.* **1970**, *53*, 124.
[36] N. F. Mott, A. M. Stoneham, *J. Phys. C: Solid State Phys.* **1977**, *10*, 3391.